3041.03

Abbreviated title: Threshold level for myelin cell transplant therapy

Title: Stem cell derived therapeutic myelin repair requires 7% cell replacement

Authors: Mary E. Kiel[1], Cui P. Chen[1], Dorota Sadowski[1] and Randall D. McKinnon[1,2]

Addresses: (1) Department of Surgery (Neurosurgery)
UMDNJ-Robert Wood Johnson Medical School,
675 Hoes Lane, Piscataway NJ 08854

(2) Dept of and Molecular Genetics Microbiology
and Member, The Cancer Institute of New Jersey

Corresponding author:
Randall D. McKinnon
UMDNJ-Robert Wood Johnson Medical School
675 Hoes Lane, S-225, Piscataway NJ 08854
tel (732) 235-4419
mckinnon@umdnj.edu

Disclaimers: The authors declare no conflicts or competing financial interests.

Key Words: Cell transplantation, Embryonic stem cells, Glia, Oligodendrocytes, Thresholds

Authors' contributions:

Mary E. Kiel: Conception and design, collection and assembly of data, data analysis and interpretation, manuscript writing;

Cui P. Chen: collection and assembly of data, manuscript writing;

Dorota Sadowski: collection and assembly of data;

Randall D. McKinnon: Conception and design, financial support, data analysis and interpretation, manuscript writing, final approval of manuscript.

Abstract

Embryonic stem (ES) cells hold great potential for therapeutic regeneration and repair in many diseases. However, many challenges remain before this can be translated into effective therapy. A principal and significant limit for outcome evaluations of clinical trials is to define the minimal graft population necessary for functional repair. Here we used a preclinical model for quantitative analysis of stem cell grafts, with wild-type ES cells grafted into myelin mutant shiverer hosts, to determine minimum graft levels for therapeutic benefit. Using a timed motor function test we identified three groups including recipients indistinguishable from non-grafted shiverer controls (t = 22.5± 1.1 sec), mice with marginal improvement (t = 15.6±1 sec), and mice with substantial phenotype rescue (t = 5.7±0.9 sec). The motor function rescued chimeras also had a considerably extended life span (T_{50}>128 days) relative to both shiverer (T_{50}=108 days) and the non-rescued chimeras. Retrospective genotype analysis identified a strong correlation (r^2 = 0.82) between motor function and ES-derived chimerism, with >7% chimerism required for rescue in this murine model of CNS myelin pathology. These results thus set the bar for minimal cell replacement to anticipate repair of cell autonomous defects by cell transplant therapy.

Introduction

Cell and organ transplant therapy is an established approach in clinical medicine, although the number of conditions that can be addressed using these therapies are relatively limited. The gold standard for cell transplants is in hematopoesis, where bone marrow stem cells from histo-compatible donors can replace those in a cancer patient. These successes have fueled the drive to apply stem cell therapy in a broad range of

genetic, acquired and degenerative diseases. Principle amongst these are clinically intractable chronic neurodegenerative conditions of the central nervous system [1] including the accumulation of β-amyloid plaques in Alzheimer's disease, the loss of dopaminergic neurons in Parkinson's disease [2] and the loss of myelin forming oligodendrocytes in multiple sclerosis (MS), the most common neurodegenerative condition of young adults [3].

There are three major hurdles to overcome before stem cell therapy can be a clinical reality for brain repair. First there is a need to identify disease mechanism in order to define the therapeutic objectives. While the mechanisms underlying Alzheimer's and Parkinson's disease remain elusive, the immune mediated loss of myelin in MS is well established, the pathology of the MS lesion is constant [3], and the repair objectives are defined [4]. The second hurdle is the need to identify an appropriate source of cells that can compensate for the cellular deficit. Potential candidates include multipotential neural stem cells [5-8], and *in vitro* derivatives of pluripotential ES cells [9-11]. ES cell technology has been extended to human cells [12] which hold great promise to regenerate any organ system for any disease [1]. However, for both neural stem and ES cells, the current technology is limited to harvesting cells from tissue sources that present significant ethical concerns. Recent advances such as the induction of pluripotent ES cells from autologous fibroblasts [13-15] have the potential to resolve these ethical concerns, as well as address the need for histo-compatible grafts. The third hurdle is the need to define how to deliver cells, and how many cells to deliver, in order to achieve therapeutic benefit. Since the brain and spinal column present tremendous surgical risks, a significant aspect of cell delivery for neural repair is to promote the migration of

grafted cells toward target lesions. This may require modifications of the grafted cells, and possibly of the host environment, in order to encourage cell homing into a lesion [4]. A second aspect is the general question of how many grafted cells are required for functional recovery [16]. In Parkinson's disease, for example, the failure of transplant therapies to date could represent insufficient numbers of grafted neural precursors [16] rather than an ineffective graft population [2].

The ability of stem cells to generate specific neural cell types has been well established in numerous preclinical transplant models. However, quantitative aspects of graft survival or extent of cell replacement have largely not been addressed to date. In the present study we examine whether the level of cell engraftment correlates with functional outcome. We chose a genetic model of CNS myelin pathology, the myelin mutant shiverer (*shi*) mice [17]. Shiverer mice lack the myelin basic protein (MBP) gene [18] and produce un-compacted myelin which subsequently degenerates (dys-myelination). This allele only affects CNS myelin, since peripheral myelin generated by Schwann cells is compacted by the P_0 protein [19]. Thus the *shi* phenotype is an effective approximation of CNS specific demyelination as seen in autoimmune mediated MS.

Shiverer mice have been used extensively for qualitative outcome evaluation of the myelin generating potential of graft cell populations, including myelin repair by ES-derived OPCs from mouse [20,21] and man [22], by neural stem cells, and by glial progenitors [23-25]. Shiverer has also been rescued by transgene approaches [26]. Here we use ES-derived cell therapy and compare functional deficits in chimeric mice with a range of wild-type stem cell-derived grafts. Our results identify limited improvements with as little as 1% engraftment, and substantial improvements in both motor function

and longevity in animals with >7% tissue engraftment. This level of cell replenishment thus sets the bar for developing effective ES-derived stem cell therapeutics. To our knowledge this is the first study to determine the minimal level of engraftment for functional neural cell replacement therapy.

Materials and Methods

Animals. Shiverer (Mbp^{shi}) mice (C3Fe.*SWV-*Mbp^{shi}/J) were obtained from Jackson Laboratory (Bar Harbor ME). Chimeras were constructed by harvesting day 3.5 MBP^{shi} blastocysts from females of homozygous (*shi/shi*) breeding pairs, injecting $Olig2^{GFP}$ ES cells (n=14 cells each), then transferring the MBP^{shi}:$Olig2^{GFP}$ chimeric blastocysts into pseudopregnant recipients (RWJMS Transgenic Core Facility). Offspring were tagged (toe) and biopsied (tail) for genotype analysis. All procedures were approved by the institutional animal care and use committee.

Cell culture. Mouse embryonic fibroblasts (MEF) were obtained from day 13 embryos of C57Bl/6J mice (Jackson Labs) using standard protocols. MEF cells were expanded for up to four passages in Dulbecco's Modified Eagle Media (DMEM, Invitrogen, Carlsbad CA) supplemented with 10% ES-tested fetal bovine serum (FBS, Atlanta Biologicals, Lawrenceville GA) and 1% non-essential amino acids (Invitrogen), using 0.25% trypsin (Invitrogen) to dissociate confluent monolayers of cells from the Falcon 3003 culture plates (Becton Dickinson, Franklin Lakes NJ). The MEF cells were γ-irradiated (4,000 rad) for mitotic arrest prior to use as ES cell feeder layers.

Olig2^{GFP} ES cells, with a green fluorescent protein (GFP) transgene in the Olig2 locus [27], were obtained from ATCC (Rockville MD). ES cells were expanded on γ-irradiated MEF, in 0.1% gelatin coated plates, in ES media (DMEM, 15% FBS, 60 uM β-mercaptoethanol, 1% non-essential amino acids) containing 100 units/mL (1.3 ng/mL) recombinant leukemia inhibitory factor (LIF, Chemicon Inc., Temecula CA).

For *in vitro* gliogenesis [4,28], ES cells were sequentially exposed to conditions that promote the formation of embryoid bodies (EB), neuroepithelial stem (NS) cells, ventral neural precursors (NP), then conditions that select for the amplification of oligodendrocyte progenitor cells (OPCs). First, ES cells were plated in nonadherent Falcon 1029 bacterial petri plates (Becton Dickinson) in ES media without LIF for 4 days to form aggregated EBs. Second, EBs were cultured for 4 days in ES media containing 500 nM retinoic acid to generate NS. Third, the NS were dissociated with trypsin and expanded for 2 days as adherent cells with 10 ng/mL basic fibroblast growth factor (FGF2, R&D Systems, Minneapolis MN) in ITSFn media [20], consisting of DMEM supplemented 5 ug/mL insulin, 50 ug/mL transferrin, 30 nM sodium selenite and 5 ug/mL fibronectin (Sigma Corp., St. Louis MO). Fourth, the NS were ventralized by exposure for 2 days the ITSFn/FGF2 media containing 300 ng/mL Sonic hedgehog (Shh, R&D Inc). Fifth, OPCs were expanded by exposure for 5 days in ITSFn containing 40 ng/mL 3,3,5 triiodothyronine (T3) plus 10 ng/mL platelet-derived growth factor (PDGF, R&D Inc). To generate oligodendrocytes (OL), OPCs were treated for 3 days in ITSFn with T3 and 0.5% FBS.

Immunocytochemistry. Monoclonal antibodies O4 [29] and RmAb [30] were obtained as supernatant fluids from the respective cell lines and polyclonal rabbit anti-MBP was from Chemicon (Temecula CA). Cells growing in Lab Tech tissue chamber slides (Nalge Nunc, Rochester NY) were fixed (room temp, 10 min) in 4% paraformaldehyde in phosphate buffered saline (PBS), washed extensively in PBS, then exposed to primary antibodies (room temp, 1 hr) diluted in PBS. The slides were then washed in PBS and exposed (room temp, 1 hr) to secondary antibodies conjugated to fluorescent (Alexa-488,Alexa-544) tags (Molecular Probes, Eugene OR). After washing in PBS the slides were mounted under coverslips in mounting media (Vector Laboratories, Burlingame CA) containing the nuclear stain 4',6'-diamidino-2-phenylindole (DAPI). Tissue sections, or whole mount spinal cords, were fixed overnight at 4°C in 4% PF then processed as above in PBS containing 0.1% triton X-100. Images were collected in 1 micron z-sections on a Zeiss LSM510 Meta confocal microscope, and assembled in Adobe Photoshop vr 6.0.

Polymerase Chain Reaction. PCR amplification was performed using an Eppendorf Mastercycler gradient thermocycler, and cycle parameters were: 95°C-2 min, 30x-(95°C-30 sec, 55°C-1 min, 72°C-2 min), 1x 72°C-10 min. The 50 ul reactions contained 1 ug genomic DNA, 0.2 uM PCR primers (Integrated DNA Technologies, Coralville IA) and Taq Polymerase (Invitrogen) with conditions specified by the manufacturer. For transcript analysis, RNA was extracted using TRIzol Reagent and copied into cDNA with M-MLV reverse transcriptase (RT) using conditions specified by the manufacturer (Invitrogen). A portion of the RT-PCR products were examined by

agarose gel electrophoresis to determine size relative to a kilobase (KB+) marker (Invitrogen). For DNA sequence analysis, RT-PCR products were purified by column chromatography (Qiagen, Valencia CA), then 50 ng DNA was subjected to automated capillary sequencing with 2 pmoles of either the forward or reverse PCR primer using an ABI PRISM 3100 Genetic Analyzer (RWJMS DNA Core Facility).

ES cell graft contribution. Chimerism was determined by real time quantitative PCR (Q-PCR) using an ABI7900HT and SDS vr2.2 software (Applied Biosystems, Foster City CA). Cycle conditions were: 50°C-2 min, 95°C-10 min, then 40 cycles of (95°C-15 sec, 55°C-15 sec, 72°C-1 min). Samples (1 ug genomic DNA) were examined in duplicate using PCR primers (Table 1) that identified wild-type MBP intron 1 and a control gene, glycerol phosphate dehydrogenase (GAPDH). The relative number of $Olig2^{GFP}$-derived cells in MBP^{shi}:$Olig2^{GFP}$ chimeric animals was determined from the threshold cycle (C_T) for PCR amplification of *mbp* intron 1 and *gapdh*, using the formula $R = 2^{-(\epsilon \epsilon C_T)}$ [31]. For each chimera, the C_T ratio (*mbp/gapdh*) was normalized to the C_T ratio of *mbp/gapdh* in wild-type (non-*shi*) animals. All Q-PCR results were compiled after completion of the functional assays, such that the motor function and longevity studies were performed in double-blind format.

Motor function, survival. Animals were tested once only on each day, and daily for 2 weeks, commencing at age 2 weeks. Motor function was determined by placing individual animals, in random order, into a small tray (3 cm height) containing water (0.5 cm depth), and recording the time for their complete exit from the tray (see Supplemental

Movie). The water tray was placed within their home cage during the testing such that the animals reunited with their litter mates upon exiting the water tray. The animal cages remained in the same room throughout the testing period in order to minimize any external influences. For survival analysis, the age of natural death was recorded for individual animals.

Statistical analyses were performed by unpaired Student's t-test and 2nd order linear regression curve fitting using SigmaPlot 8.0 (SPSS Inc.).

Results

Shiverer-Olig2^{GFP} chimerism

The classical model for assessing myelination by exogenous grafts is the dys-myelinating shiverer (MBP^{shi}) mutant mouse [17,18] with a genomic deletion that spans the *mbp* gene (Fig 1A). Homozygous shiverer mutants form uncompacted myelin which degenerates. The loss of axonal insulation causes a pronounced movement-stimulated tremor and motor impairment, first visible at 12 days of age, with tonic seizures, late onset paralysis and a shortened life span. However, shiverer nulls are both viable and fertile. The grafting of either oligodendrocytes (OL) or their immediate progenitor cells (OPC) into neonatal shiverer hosts [32,33] restores compact myelin [34] and can restore partial function [35].

Our objective was to generate a cohort of MBP^{shi}:Olig2^{GFP} chimeras, with individual animals harboring a range (low to high) of ES-derived MBP^{wt} cells. We

reasoned that the most expedient approach was to generate blastocyst chimeras, where the numbers of grafted cells that participate in organogenesis would be stochastic amongst recipients, while the contribution of ES^{wt} to the three germ layers would be relatively constant within individual chimeras. We grafted ~14 $Olig2^{GFP}$ ES cells into day 3.5 *shi/shi* blastocysts then transferred these to pseudo-pregnant foster mothers. Chimeric embryos were harvested at day 13.5 to 15.5 for histochemical studies, and we examined chimeric animals from full term litters for motor function and lifespan. There were no significant differences in the number of viable offspring in MBP^{shi}:$Olig2^{GFP}$ chimeric litters at either e13-15 (31 embryos in 3 litters) or at full term (29 pups in 4 litters), and both were equivalent to the litter size of uninjected MBP^{shi} control litters. Thus the grafted $Olig2^{GFP}$ ES cells did not appear to impact early development, consistent with an exclusively postnatal phenotype for the Mbp^{shi} allele [36].

To determine the extent of chimerism we used genomic DNA analysis, focusing on Q-PCR amplification of a chromosomal fragment that is unique to wild-type *mbp* intron 1 (Fig. 1A). Attempts to PCR amplify the chromosomal fragment spanning the MBP^{shi} deletion breakpoint were uninformative, possibly due to reiterated sequences downstream of exon 7 which appear to be responsible for the *shi* chromosomal deletion [37]. The Mbp^{wt} intron 1 PCR fragment was absent in *shi/shi* controls and present in most chimeric animals examined, with a broad range of signal strength in individual chimeras (Fig. 1B). To determine the relative level of ES-derived Mbp^{wt} in each animal, we normalized the threshold (C_T) MBP^{wt} signal to that of a control PCR product (*gapdh*), which is present at the same copy number in both MBP^{shi} (host) and $Olig2^{GFP}$ (graft) cells. The normalized *mbp* levels were then compared to normalized C_T (*mbp/gapdh*) in

wild-type (non-*shi*) animals (Table 2). This analysis revealed a range of chimerism from undetectable through 26% Olig2^{GFP}. We did not detect any obvious bias for ES contribution to distinct germ layers in individual chimeras. Relative to brain (1.00), the levels of Olig2^{GFP} derived cells was comparable in heart (1.02), kidney (.87), liver (.62), skeletal muscle (.70) and tail (.99). Importantly, the genomic analysis was performed subsequent to the functional studies described below, and all Q-PCR results were complied post-hoc so that the functional outcome was performed in double blind format.

Shi-Olig2^{GFP} chimeras express MBP

To determine whether the ES cells used (Olig2^{GFP}) could generate MBP^{+} oligodendrocytes we examined both transcript and protein expression (Fig. 2). For *in vitro* differentiation the cells were first aggregated into embryoid bodies then sequentially exposed to neural induction factors (RA, FGF, Shh) followed by glial cell mitogens (FGF, PDGF) as detailed in Methods. This process generated cells with the characteristic morphology and marker profile of lineage committed OPCs and OLs (Fig. 2A), and these were indistinguishable from *bona fide* OL lineage cells isolated from the neonatal rodent brain [38]. Thus the G-olig2 cells were competent to generate OL-lineage cells *in vitro*.

To determine if ES^{wt}-derived cells had undergone OL differentiation *in vivo*, we examined the expression of MBP transcripts (Fig. 2B) and protein (Fig. 2C-E) in MBP^{shi}:Olig2^{GFP} chimeras. Using RT-PCR, MBP transcripts were observed in most chimeras examined (Fig. 2B, center panels), including both embryonic day 14 (lanes 14a-d) and day 15 (lanes 15a-d). The predominant MBP transcripts were splice variants lacking exon 2, and for several animals we also observed a smaller, earlier emerging

transcript lacking exons 2 and 6 (lanes 14a, 15a). No MBP transcripts were detected in non-grafted shiverer control animals. OL lineage differentiation of graft-derived cells was also confirmed by expression of hybrid Olig2-green fluorescent protein (GFP) transcripts (Fig. 2B, top panels). Olig2^{GFP} cells have the *gfp* transgene inserted within the *olig2* locus, with GFP expression controlled by the endogenous *olig2* cis-regulatory elements [27]. Thus the onset of GFP expression marks the activation of endogenous Olig2, an early marker for OPC fate induction [39]. Consistent with this, hybrid Olig2-GFP transcripts were detected in chimeras that expressed early isoforms of MBP, lacking both exons 2 and 6 (Fig. 2B, lanes 14a, 15a).

Using histochemistry we also detected MBP^{+} OLs in whole mount spinal cord preparations of embryonic MBP^{shi}:Olig2^{GFP} chimeras (Fig. 2C-E). MBP staining was completely absent from shiverer controls. In a single chimera we detected an asymmetric (mosaic) distribution of MBP in the rostral spinal cord (Fig. 2C). MBP^{+} OLs were absent from the left and present on the right side of this cord (Fig. 2C). Thus at least some regions of the chimeric neural tube could be generated exclusively from host-derived (MBP^{shi}) cells. This likely represents a stochastic partitioning of grafted ES cells within this neural tube, since our genomic analysis did not identify a bias in contribution of grafted cells to different germ layers. Together with the transcript analysis above, these studies demonstrate that the grafted Olig2^{GFP} ES cells were competent to generate MBP^{+} OLs in MBP^{shi}:Olig2^{GFP} chimeric animals.

Motor function analysis

The shiverer motor tremor first appears at postnatal day 10-12, at the peak of brain myelination, and there are many functional tests that can identify the differences between wild-type and shiverer mice. To address whether Olig2^{GFP} ES cell grafts affected the *shi* phenotype, and to quantify any such effects, we developed a sensitive water avoidance assay for motor function (Fig. 3). Beginning at 2 weeks of age, and daily for 2 weeks, animals were placed in a shallow water tray within their home cage and the time required for exit was recorded (Supplemental movie: water avoidance.avi). Wild type mice had no difficulty in this test, with an exit speed of 5.5±0.6 sec (Table 2). *Shi* control mice, in contrast, had poor motor coordination, difficulty balancing on the tray edge, and an overall slow exit time from this hostile environment (t=22.5±1.1 sec, 92 events). There was no obvious deterioration in their motor function over the trial period (Fig. 3A, solid symbols).

In the MBP^{shi}:Olig2^{GFP} chimera cohort, one animal had obvious coat color chimerism and an absence of shiver, while all other chimeras retained an obvious tremor and were not readily distinguishable from shiverer controls. However, all MBP^{shi}:Olig2^{GFP} chimeras displayed a range of performance ability in the motor function test. Animals were tested in random order on each test day, and subsequent decoding of the results revealed three groups of motor function performance. Of note, all three groups had poor motor performance on the first three days of testing. Group I mice (Fig. 3A, open symbols) performed essentially identical (t=20.1 ± 2.5 sec, 44 events) to the non-grafted *Shi* controls (p=0.34) throughout the testing period. A second group (II) showed an overall 21.6% faster exit time (t=15.6 ± 1.0, 69 events, p<0.001) relative to *Shi* controls, and the difference with *shi* was most apparent towards the latter test days (Fig.

3B). A third group (III) had a 74.5% faster exit speed (t=5.7 ± 0.9, 31 events), significantly faster ($p<0.0001$) than the *Shi* controls and essentially equivalent to wild-type (non-shiverer) levels (Fig. 3C). Thus the motor function test as used here identified subtle difference in balance and coordination between chimeras and *shi/shi* mutant animals. The consistency of motor performance for animals in each group during the testing period suggests this analysis was an effective metric for the $Olig2^{GFP}$ engraftment levels in these chimeras.

MBP chimerism correlates with motor function

We next decoded the genomic chimerism data, the results of which identified a strong and surprising correlation ($r^2 = 0.82$) of MBP^{wt} levels to motor performance (Fig. 4). Group I chimeras, which were not significantly faster than age-matched Shi mutants, had less than 0.1% of wild-type cells. Group II chimeras with 22% faster exit speed contained between 0.1-5% wild-type cells. Group III chimeras, with 75% faster exit speed, contained greater than 7% wild-type cells (Fig. 4). Two groups of outliers were excluded from this correlation. One animal showed relatively fast avoidance time (t=10 sec) with a low level of detectable chimerism, while two animals with higher levels of chimerism performed poorly in the functional assay (Fig. 4). Since the results of this study were decoded after the longevity analysis (see below), we were unable to determine if these outliers represent either germ layer or CNS region-specific mosiac distribution of $Olig2^{GFP}$ grafted cells.

MBP chimerism correlates with longevity

Finally we addressed the effect of chimerism on longevity. Age of natural death was recorded for each animal and the survival curves were tabulated for each of the three groups of cohorts (Fig 5). Shi mutants and chimeras with lower levels of wild-type cells (groups I, II) had a relatively short natural life span with 50% mortality (T_{50}) of 108 days (Fig. 5). In sharp contrast, group III chimeras with greater than 7% wild-type ES cells had a considerably extended lifespan (T_{50}>128 days). This rather striking correlation was only revealed after the death of all but one animal (H5), who has remained viable as of 550 days. Back crossing this female to a MBP^{shi} male generated one litter, and all F_1 offspring were homozygous *shi/shi*, consistent with the finding that the parental ES cells are not germ line competent [27].

Discussion

One limitation to evaluating the outcome of cell transplants has been defining the minimal graft level required for tissue repair and therapeutic recovery. Indeed, the efficiency of cell engraftment has not been addressed in most cell transplant models to date. Here we used quantitative genomic analysis to measure chimerism, and we identify a strong correlation between levels of engraftment and functional benefits of ES-derived CNS myelin replenishment therapy. At 1% wild-type engraftment there is a small but significant increase in motor function, and above 7% engraftment there are significant improvements in both motor function and longevity. These results thus establish the minimal levels of graft replacement for therapeutic outcome in a cell autonomous deficit.

The experimental model we have used, dysmyelinating shiverer mice, has several advantages for this type of analysis. First, the pathology of shiverer mice is limited to the

CNS and is distributed throughout the brain and spinal cord. The shiverer animals described in this study were maintained on a common genetic background, and there is no detectable phenotype variation between individual *shi/shi* animals. Second, grafting cells into day 3.5 blastocysts allowed us to deliver a standard number of donor cells to each chimera. The ES donor cells were expanded under standard culture conditions, and transplants were performed using a reproducible approach, minimizing any potential variations in both host and graft cell populations. Thus variations in phenotype of the resultant chimeras are a consequence of differences in the numbers of grafted cells that contribute to organogenesis.

One underlying assumption in this study is that individual chimeras with different levels of $Olig2^{GFP}$ engraftment have an equal distribution of graft-derived cells throughout their CNS. The strong correlation observed between motor function and level of engraftment (Fig. 4) lends credibility to this assumption. However this does not eliminate all concerns, and we did find one example of asymmetry in the distribution of MBP-positive cells in the spinal column (Fig. 2C). It is attractive to speculate that a mosaic dis-equilibrium in graft distribution underlies the animals who did not fit into our regression analysis (Fig. 4). Whether such outliers reflect an uneven graft distribution requires a detailed analysis which we were not able to address in the present study.

Another question that remains unresolved is what level of compact myelin restoration is necessary for functional rescue. MS patients have a range of symptoms from subtle such as temperature sensitivity to extreme including motor impairment. It is conceivable that lower levels of engraftment and compact myelin restoration could be sufficient, or higher levels necessary, for repair of distinct deficits. Here we focused on

general motor function in the shiverer model, and we have not examined other functional outputs. In shiverer the myelin deficit affects the entire CNS, while demyelinated regions in MS or spinal cord injury involved localized regions or plaques. It is of note that the size of a typical MS plaque can be very large, and the levels of cell replacement required to repair such lesions would likely parallel the order of magnitude required to repair the shiverer brain.

Conclusions/Summary

The current focus of MS therapy is immune suppression [40]. This is not a cure, and its efficacy remains controversial [41]. There is a need for new therapeutic strategies, and the use of cell transplants is supported by preclinical studies [4]. However for clinical transplants to be effective they must meet significant hurdles, including avoiding the sensitized immune environment of the MS patient. Thus allografts would require sustained immune suppression and may do more harm than good. In contrast, autologous grafts of either adult stem cells or reprogrammed somatic cells [13,42] as an emerging field represents a potential and promising alternative. To realize this potential it will be necessary to address hurdles such as targeting the migration of grafted cells towards lesions [4]. Our present results suggest that evaluating the efficacy of alternative graft sources, or the homing of grafted cells into demyelinated lesions, should be evaluated on the criteria of a minimum of 7% replacement for functional improvement.

Acknowledgments: We thank Drs. Mantu Bhaumik and Jack Spychala of the Transgenic and DNA Core Facilities for their support. Supported by grants from the New Jersey

Commission on Spinal Cord (05-3047-SCR-E-0) and Stem Cell (06-2042-014-74) Research, and US Public Health Service Grant MH54652 from the National Institute of Mental Health.

References

1. Lindvall O, Kokaia Z. Stem cells for the treatment of neurological disorders. **Nature** 2006; 441:1094-1096.

2. Bjorklund A, Dunnett SB, Brundin P et al. Neural transplantation for the treatment of Parkinson's disease. **Lancet Neurology** 2003; 2:437-445.

3. Frohman EM, Racke MK, Raine CS. Medical progress: Multiple sclerosis - The plaque and its pathogenesis. **New England Journal of Medicine** 2006; 354:942-955.

4. Chen CP, Kiel ME, Sadowski D, McKinnon RD. From stem cells to oligodendrocytes: prospects for brain therapy. **Stem Cell Reviews** 2007; 3:280-288.

5. Reynolds RA, Weiss S. Generation of neurons and astrocytes from isolated cells of the adult mammalian central nervous system. **Science** 1992; 255:1707-1710.

6. Davis AA, Temple S. A Self-Renewing Multipotential Stem-Cell in Embryonic Rat Cerebral-Cortex. **Nature** 1994; 372:263-266.

7. Morshead CM, Reynolds BA, Craig CG et al. Neural stem cells in the adult mammalian forebrain: a relatively quiescent subpopulation of subependymal cells. **Neuron** 1994; 13:1071-1082.

8. Uchida N, Buck DW, He DP et al. Direct isolation of human central nervous system stem cells. **Proc Natl Acad Sci USA** 2000; 97:14720-14725.

9. Evans MJ, Kaufman MH. Establishment in Culture of Pluripotential Cells from Mouse Embryos. **Nature** 1981; 292:154-156.

10. Martin GR. Isolation of a pluripotent cell line from early mouse embryos cultured in medium conditioned by teratocarcinoma stem cells. **Proc Natl Acad Sci USA** 1981: 78;7634-7638.

11. Bradley A, Evans M, Kaufman MH, Robertson E. Formation of Germ-Line Chimeras from Embryo-Derived Teratocarcinoma Cell-Lines. **Nature** 1984: 309;255-256.

12. Thomson JA, Itskovitz-Eldor J, Shapiro SS et al. Embryonic stem cell lines derived from human blastocysts. **Science** 1998: 282;1145-1147.

13. Takahashi K, Yamanaka S. Induction of pluripotent stem cells from mouse embryonic and adult fibroblast cultures by defined factors. **Cell** 2006: 126;663-676.

14. Wernig M, Meissner A, Foreman R et al. In vitro reprogramming of fibroblasts into a pluripotent ES-cell-like state. **Nature** 2007: 448;318-324.

15. Okita K, Ichisaka T, Yamanaka S. Generation of germline-competent induced pluripotent stem cells. **Nature** 2007: 448;313-3U1.

16. Freed CR, Breeze RE, Greene P et al. Transplanted dopaminergic neurons: More or less? Reply. **Nature Med** 2001: 7;12-513.

17. Bird TD, Farrell DF, Sumi SM. Genetic developmental myelin defect in shiverer mouse. **Trans Am Soc Neurochem** 1977: 8;153.

18. Jacque C, Privat A, Dupouey P et al. Shiverer mouse: a dysmyelinating mutant with absence of major dense line and basic protein in myelin. **Proc Eur Soc Neurochem** 1978: 1;131.

19. Pfeiffer SE, Warrington AE, Bansal R. The oligodendrocyte and its many cellular processes. **Trends in Cell Biology** 1993: 3;191-197.

20. Brustle O, Jones KN, Learish RD et al. Embryonic stem cell-derived glial precursors: A source of myelinating transplants. **Science** 1999: 285;754-756.

21. Perez-Bouza A, Glaser T, Brustle O. ES cell-derived glial precursors contribute to remyelination in acutely demyelinated spinal cord lesions. **Brain Pathology** 2005: 15;208-216.

22. Keirstead HS, Nistor G, Bernal G et al. Human embryonic stem cell-derived oligodendrocyte progenitor cell transplants remyelinate and restore locomotion after spinal cord injury. **J Neurosci** 2005: 25;4694-4705.

23. Groves AK, Barnett SC, Franklin RJM et al. Repair of demyelinated lesions by transplantation of purified O-2A progenitor cells. **Nature** 1993: 362;453-455.

24. Warrington AE, Barbarese E, Pfeiffer SE. Stage specific, (O4+GalC-) isolated oligodendrocyte progenitors produce MBP+ myelin in vivo. **Dev Neruosci** 1992: 14;93-97.

25. Tontsch U, Archer DR, Dubois-Dalcq M, Duncan ID. Transplantation of an oligodendrocyte cell line leading to extensive myelination. **Proc Nat'l Acad Sci USA** 1994: 91;11616-11620.

26. Readhead C, Popko B, Takahashi N et al. Expression of a myelin basic protein gene in transgenic shiverer mice: correction of the dysmyelinating phenotype. **Cell** 1987: 48;703-712.

27. Xian HQ, McNichols E, St Clair A, Gottlieb DI. A subset of ES-cell-derived neural cells marked by gene targeting. **Stem Cells** 2003: 21;41-49.

28. Billon N, Jolicoeur C, Ying QL et al. Normal timing of oligodendrocyte development from genetically engineered, lineage-selectable mouse ES cells. **Journal of Cell Science** 2002: 115;3657-3665.

29. Sommer I, Schachner M. Monoclonal antibodies (01 to 04) to oligodendrocyte cell surfaces: an immunocytological study in the central nervous. **Dev Bio** 1981: 83;311-327.

30. Ranscht B, Clapshaw PA, Price J et al. Development of oligodendrocytes and Schwann cells studied with a monoclonal antibody against galactocerebroside. **Proc Nat'l Acad Sci USA** 1982: 79;2709-2713.

31. Livak KJ, Schmittgen TD. Analysis of relative gene expression data using real-time quantitative PCR and the 2(T)(-Delta Delta C) method. **Methods** 2001: 25;402-408.

32. Gumpel M, Baumann N, Raoul M, Jacque C. Survival and differentiation of oligodendrocytes from neural tissue transplanted into new-born mouse brain. **Neurosci Lett** 1983: 37;307-311.

33. Lachapelle F, Gumpel M, Baulac M et al. Transplantation of CNS fragments into the brain of shiverer mutant mice: Extensive myelination by implanted oligodendrocytes. I. Immunohistochemical Studies. **Develop Neurosci** 1983: 6;325-334.

34. Gansmuller A, Lachapelle F, Baron-Van Evercooren A et al. Transplantation of newborn CNS fragments into the brain of shiverer mutant mice: extensive myelination by transplanted oligodendrocytes. II. electron microscopic study. **Develop Neurosci** 1986: 8;197-207.

35. Kuhn PL, Petroulakais E, Zazanis GA, McKinnon RD. Motor function analysis of myelin mutant mice using a rotarod. **Int J Devel Neurosci** 1995: 13;715-722.

36. Chernoff GF. Shiverer: an autosomal recessive mutant mouse with myelin deficiency. **J Hered** 1981: 72;128.

37. Molineaux SM, Engh H, De Ferra F et al. Recombination within the myelin basic protein gene created the dysmyeinating shiverer mouse mutation. **Proc Nat'l Acad Sci USA** 1986: 83;7542-7546.

38. McKinnon RD, Smith C, Behar T et al. Distinct effects of bFGF and PDGF on oligodendrocyte progenitor cells. **Glia** 1993: 7;245-254.

39. Lu QR, Sun T, Zhu Z et al. Common developmental requirement for olig function indicates a motor neuron/oligodendrocyte connection. **Cell** 2002: 109;75-86.

40. Vogel F, Hemmer B. New immunomodulatory treatment strategies in multiple sclerosis. **Nervenheilkunde** 2002: 21;508-511.

41. Marrie RA, Rudick RA. Drug Insight: interferon treatment in multiple sclerosis. **Nature Clinical Practice Neurology** 2006: 2;34-44.

42. Wakayama T, Tabar V, Rodriguez I et al. Differentiation of embryonic stem cell lines generated from adult somatic cells by nuclear transfer. **Science** 2001: 292;740-743.

Table 1. Oligonucleotide primers for PCR amplification.

Gene	NCBI ID	Primers
GAPDH:	BC083080	5'-agccaaaagggtcatcatctc
		5'-ctgtggtcatgagtccttcca
MBP (intron 1):	AC158975	5'-gaggccgcacatcagccctgattttgctaag
		5'-gataggactggcctctgctgctt
		5'-ctcaccgtcctgagaccatt
		5'-cactgtctccaggggaagaa
G-olig2:	AB038697	5'-ttacagaccgagccaacacc
	U55762	5'-ttgaattcttacttgtacagctcgtcc

PCR primer pairs for *gapdh*, *mbp* intron 1 and the hybrid *Olig2-GFP* locus of Olig2^{GFP}. The primers listed for *mbp* intron 1 represent nested sets, and for G-olig2 the forward primer identifies *Olig2* and the reverse primer corresponds to *GFP* sequences.

Table 2. MBP^{shi}:$Olig2^{GFP}$ chimerism, water avoidance.

	C_T (GAPDH)	C_T (MBP)	% wild-type	Time (sec)
MBP^{wt}	25.07 ± 0.78	22.21 ± 0.72	100	5.47 ± 0.59
MBP^{shi}	25.58 ± 1.64	n.d.	0.00	22.47 ± 1.17
MBP^{shi}:$Olig2^{GFP}$				
F5	22.10 ± 0.23	31.83 ± 0.99	0.02%	19.58 ± 4.58
G7	22.79 ± 0.17	32.5 ± 1.15	0.02%	9.58 ± 2.24
G8	24.21 ± 0.85	32.54 ± 0.83	0.04%	16.03 ± 5.29
G5	23.94 ± 0.32	32.2 ± 1.82	0.04%	21.35 ± 4.31
F7	23.94 ± 0.48	32.1	0.05%	14.48 ± 2.68
F9	25.79 ± 0.25	32.89	0.10%	23.72 ± 5.22
G2	24.51 ± 0.19	31.33	0.12%	22.78 ± 3.42
F6	24.60± 0.45	31.14 ± 2.63	0.15%	22.29 ± 5.26
F8	23.15 ± 0.35	29.48 ± 0.57	0.17%	16.17 ± 2.41
G4	24.61 ± 0.34	30.83 ± 0.56	0.18%	10.85 ± 2.10
G3	25.47 ± 0.29	29.66 ± 0.67	0.75%	15.09 ± 2.58
F4	22.24 ± 0.45	26.16 ± 0.17	0.91%	14.12 ± 2.13
H6	22.15 ± 0.38	23.04 ± 0.65	1.62%	13.83 ± 2.71
F2	21.76 ± 0.19	24.11 ± 0.15	2.69%	11.48 ± 2.64
H3	22.55 ± 0.26	23.6 ± 1.05	6.63%	17.97 ± 3.40
G6	24.42 ± 0.73	24.92 ± 0.58	7.25%	5.79 ± 1.35
H2	24.67 ± 0.32	24.65 ± 0.97	13.91%	20.46 ± 3.29
H4	25.08 ± 0.63	24.96 ± 2.24	14.99%	17.05 ± 2.73
H1	24.34 ± 1.32	24.2 ± 2.16	15.16%	15.57 ± 3.02

H7	23.59 ± 0.59	23.24 ± 2.54	17.53%	14.21 ± 2.64
H5	22.99 ± 1.05	22.07 ± 0.80	26.00%	5.27 ± 1.31
G1	22.87 ± 0.34	21.95 ± 1.13	26.05%	5.09 ± 1.28

Q-PCR analysis of *MBP*^{wt} (n=8), MBP^{shi} (n=11), and individual MBP^{shi}:Olig2^{GFP} chimeric mice, listed by level of MBP^{wt} chimerism. C_T: threshold cycle (mean ± s.d.) from n=2-5 independent replicates. Chimerism (% wild-type) was determined by comparing C_T of *mbp* (normalized to *gapdh*) for chimeric animals to normalized *mbp* in wild-type animals (100%). Exit times (mean ± s.d.) from a water basin were recorded once daily for two weeks.

Figure 1. MBP genomic analysis. (**A**) The *mbp*^{shi} deletion. PCR primers (arrows) spanning the intron 1 deletion breakpoint were used to quantitate Olig2^{GFP}-derived wild-type cells in chimeric animals. (**B**) PCR products for *mbp* and *gapdh* in individual chimeric animals (C1-H7) and wild type (wt) controls.

Figure 2. Olig2^{GFP}-derived OLs, *in vitro* and *in vivo*. (**A**) OLs *in vitro*. (**B**) RT-PCR analysis of e14-15 spinal cords; primers are shown as arrows on exon maps (left). (**C**) MBP^{+} OLs in e15 chimera spinal cord; ventral midline is center. (**D**) Dorsal horn of the same cord. (**E**) Olig2^{GFP}-derived myelin sheaths attached to OL soma.

Figure 3. Exit times for *Mbp*^{shi} mutants (solid symbols) and for MBP^{shi}:Olig2^{GFP} chimeras (open symbols), including (**A**) group-I, (**B**) group-II, and (**C**) group-III chimeras. Both group II and III chimeras were significantly faster ($p<.001$) than *Mbp*^{shi}, while group I chimeras was not ($p=0.34$). Motor function was scored in double-blind format with genotype analysis decoded post hoc.

Figure 4. Correlation between chimerism and motor function. Chimerism was determined by cycle threshold (C_T) using Q-PCR analysis of genomic DNA, with *mbp* levels normalized to *gapdh* control then compared to normalized *mbp* in wild-type animals. Motor function was as outlined in Fig. 3.

Figure 5. Survival of MBP^{shi}:Olig2^{GFP} chimeras. Age of natural death for MBP^{shi} (circles) and for MBP^{shi}:Olig2^{GFP} chimeras from group II (triangles) and III (square symbols). Group III chimeras with >20% extended life span relative to MBP^{shi} controls retained a mild tremor.

Fig 1. McKinnon (top)

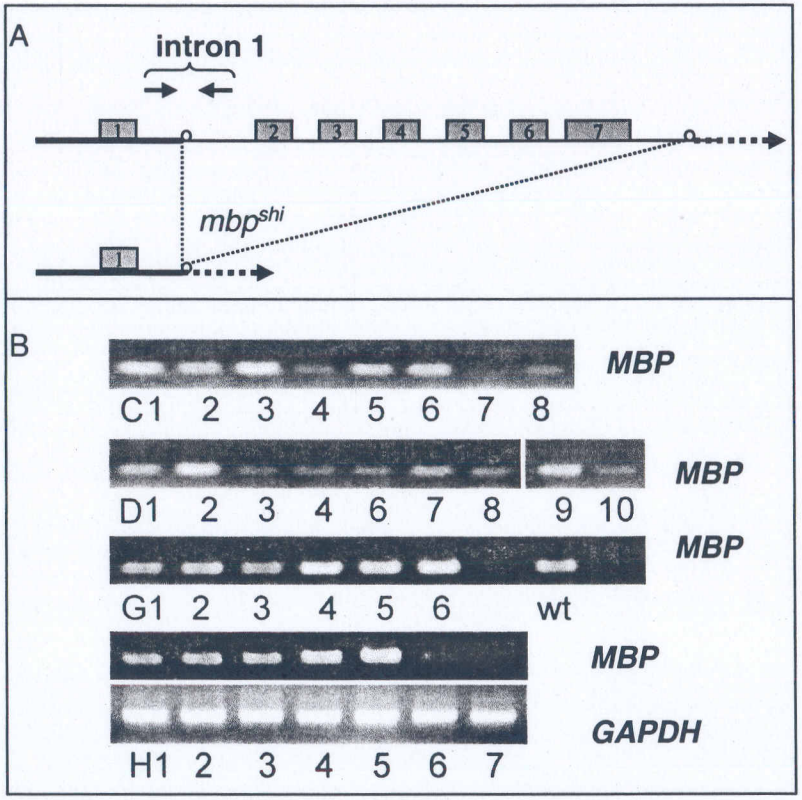

Fig 2. McKinnon (top)

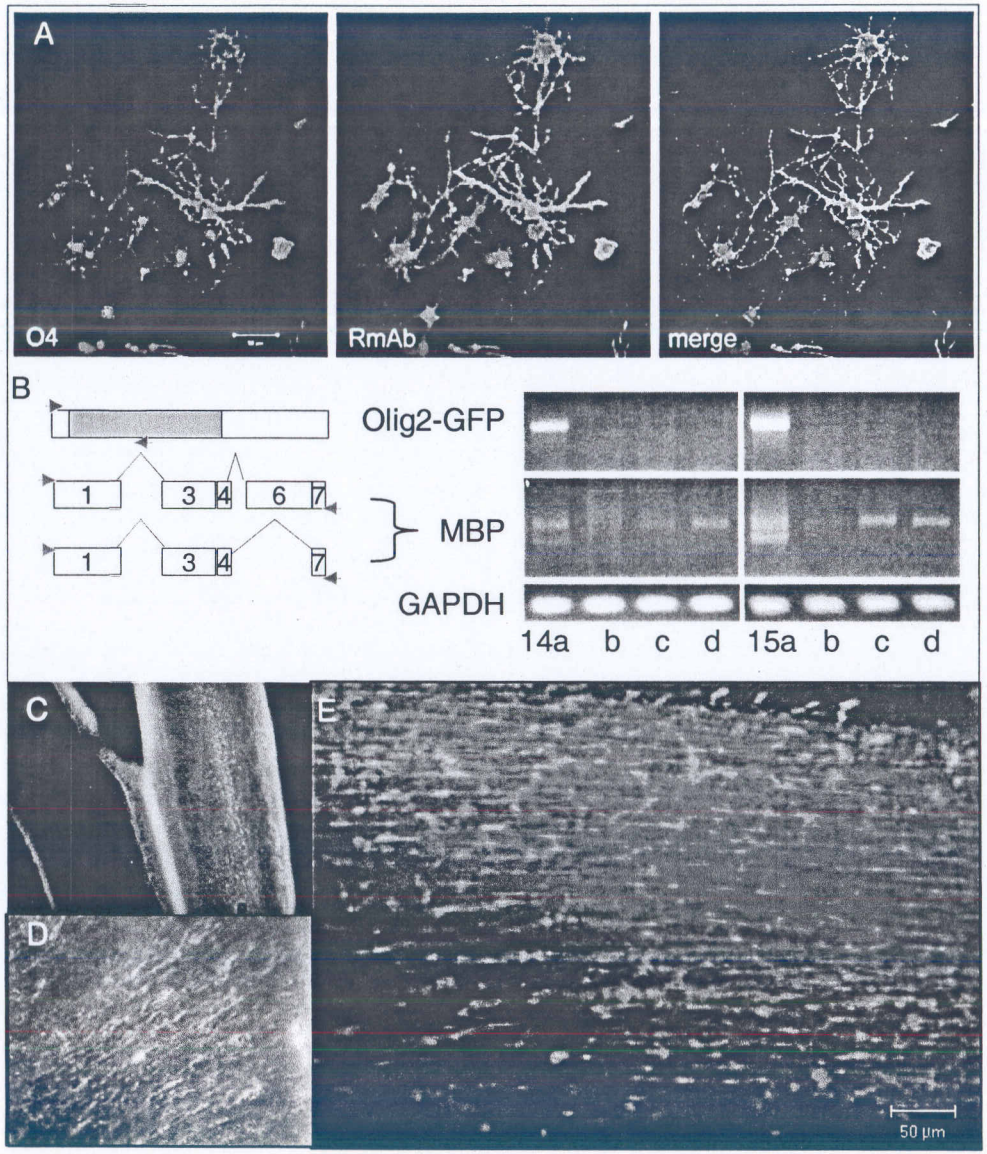

Fig 3. McKinnon (top)

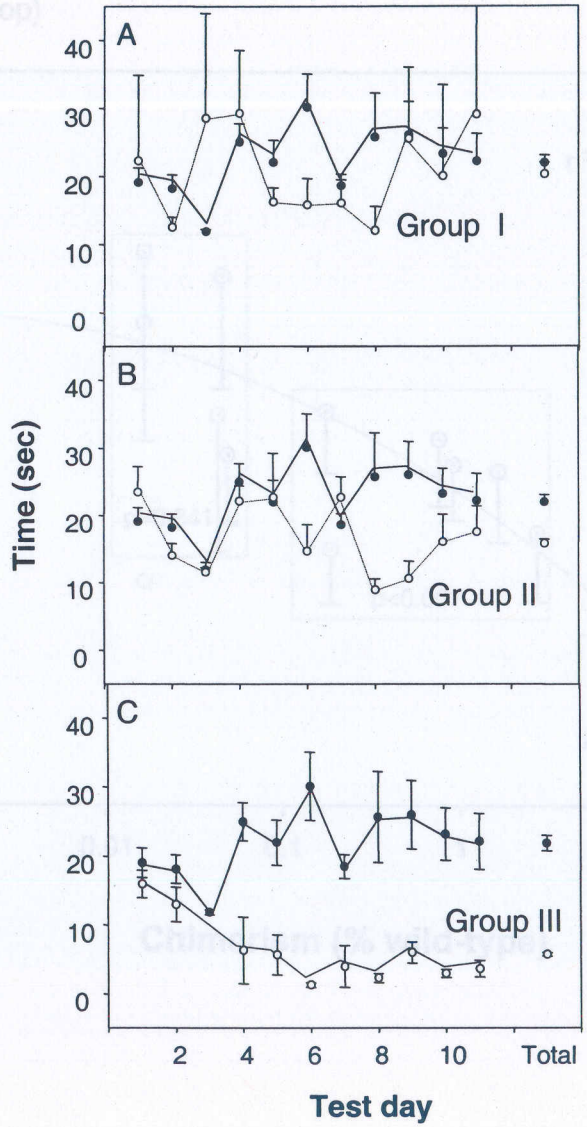

Fig 5. McKinnon (top)